Auger-electron study of correlation effects in $5s^05p^6$ and $5s^15p^5$ configurations of xenon

H. Aksela, S. Aksela, and H. Pulkkinen
Department of Physics, University of Oulu, SF-90570 Oulu 57, Finland
(Received 12 September 1983)

The $4d^9 \rightarrow 5s^05p^6$, $4d^9 \rightarrow 5s^15p^5$, and $4d^9 \rightarrow 5s^25p^4$ Auger transitions of xenon have been studied both experimentally and theoretically. Final states of these transitions are found to be affected by strong electron correlation effects. Results from Auger-electron spectra are compared with the corresponding results of optical spectroscopy and with the theoretical estimates based on Dirac-Fock multiconfiguration computations.

I. INTRODUCTION

The experimental $N_{4,5}OO$ Auger spectrum of xenon was published by Werme *et al.*[1] together with some other Auger spectra of noble gases. The spectra were also interpreted tentatively. A reassignment of some lines in the $L_{2,3}MM$ spectrum of argon and in the $M_{4,5}NN$ spectrum of krypton was reported by McGuire[2,3] and later confirmed by Dyall and Larkins.[4,5] Correlation between the final states of the normal and the satellite transitions was found to cause considerable shifts in the energy positions of the normal Auger lines of argon. A similar situation is also possible in the $N_{4,5}OO$ Auger spectrum of xenon. Strong satellite structure in the $5s$-$5p$ photoelectron spectrum of xenon has already been observed and analyzed.[6,7]

The energy-level structure of the $5s^05p^6$, $5s^15p^5$, and $5s^25p^4$ configurations of xenon was recently studied by Hansen *et al.*[8,9] His analysis was based on optical data and their comparison with the Auger electron results of Werme *et al.*[1] and the electron impact excited vacuum ultraviolet (vuv) emission results of Hertz.[10] In order to carry out a detailed investigation on the $N_{4,5}OO$ Auger spectrum of xenon, we decided to remeasure the spectrum and calculate the transition energies applying a multiconfiguration Dirac-Fock (DF) method.[11] The experimental results were then compared with the earlier experimental results of Werme *et al.*,[1] with the optical results[8–10] as well as with the theoretical calculations.

While we were preparing our final results for publication, a paper by Southworth *et al.*[12] was published in which an assignment of the $N_{4,5}OO$ Auger spectrum of Xe was also proposed. We found it extremely interesting to compare our present results and calculations with their results, which were obtained with the use of synchrotron radiation.

II. EXPERIMENTAL

The $N_{4,5}OO$ spectrum of Xe was measured by means of a cylindrical mirror spectrometer and with the use of electron-beam excitation.[13] In order to increase the counting efficiency for these low energies, the electrons were accelerated by 20 eV before the analyzer using a simple grid system. A standard pulse counting method was used and the pulses were collected into the memory of a microprocessor, which was also used to control the spectrometer.

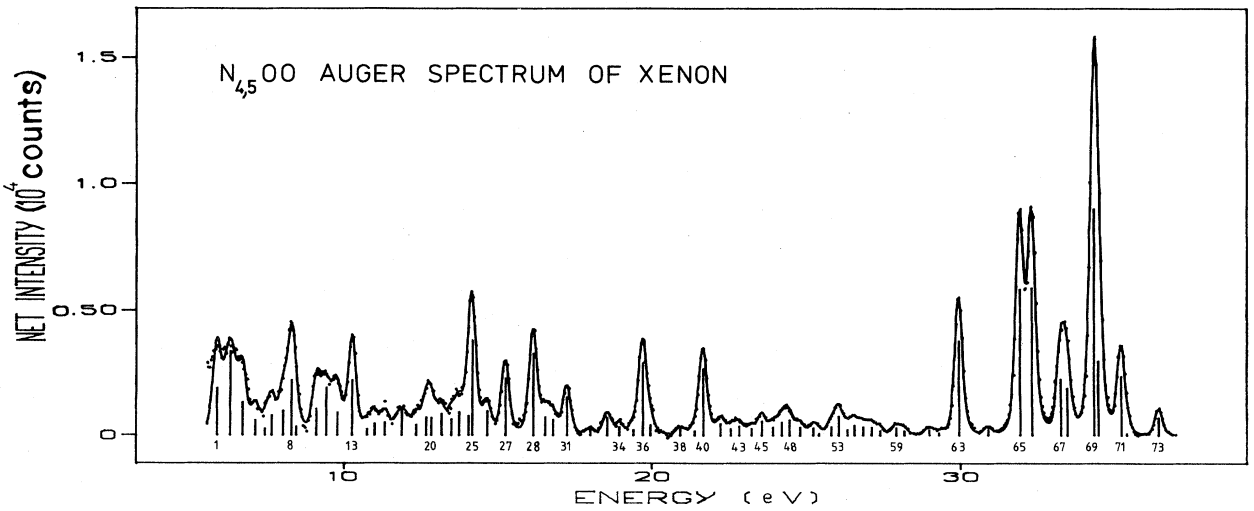

FIG. 1. Experimental Auger-electron spectrum of xenon after background subtraction. The solid curve and the vertical lines represent a least-squares fit of Voight functions to the experimental points.

TABLE I. Energies of the observed lines in the electron spectrum of xenon at the energy region 5–40 eV.

This work		Werme *et al.*		This work		Werme *et al.*	
Line number in Fig. 1	Energy (in eV)	Line number in Fig. 7 of Ref. 1	Energy (in eV)	Line number in Fig. 1	Energy (in eV)	Line number in Fig. 7 of Ref. 1	Energy (in eV)
1	5.87			38	20.92		
2	6.31			39	21.39	17	21.33
3	6.72			40	21.67	16	21.68
4	7.14			41	22.23	15	22.28
5	7.45			42	22.56		
6	7.67			43	22.84		
7	8.03			44	23.24		
8	8.30	30	8.32	45	23.57	14	23.58
9	8.46			46	23.93		
10	9.11			47	24.22		
11	9.44			48	24.46	13	24.27
12	9.80			49	24.81		
13	10.27	29	10.31	50	25.24		
14	10.76			51	25.42		
15	11.01			52	25.82		
16	11.34			53	26.06	12	25.96
17	11.89			54	26.34	11	26.17
18	12.35			55	26.56	10	26.59
19	12.68			56	26.84		
20	12.85	28	12.78	57	27.12		
21	13.16			58	27.40		
22	13.50			59	27.92		
23	13.76			60	28.18		
24	14.06			61	28.97		
25	14.18	27	14.19	62	29.30		
26	14.66	26	14.72	63	29.95	9	29.97
27	15.26	25	15.29	64	30.89		
28	16.15	24	16.16	65	31.93	8	31.95
29	16.54			66	32.31	7	32.33
30	16.80			67	33.24	6	33.23
31	17.25	22	17.26	68	33.45	5	33.45
32	18.00			69	34.31	4	34.31
33	18.55			70	34.46	3	34.45
34	18.94	20	18.98	71	35.20	2	35.23
35	19.40	19	19.31	72	35.37		
36	19.71	18	19.69	73	36.41	1	36.44
37	19.95						

Energy calibration was carried out with the aid of the $N_4O_{2,3}O_{2,3}(^1D_2)$ and $N_4O_1O_{2,3}(^1P_1)$ Auger lines of Xe with energies of 34.312 and 21.674 eV, respectively.[14] These lines were chosen as the calibration lines because they are well separated in the experimental spectrum. The corresponding lines of the N_5 group recommended by Hansen[9] overlap with the other lines, making their use as the calibration lines less reliable. The spectrum has not been corrected for the varying transmission of the spectrometer. This is because no intensity analysis is carried out in this work.

In addition to the subtraction of a constant background, a background shape increasing strongly towards the low-energy side and approximated by a polynomial was also subtracted before decomposition of the experimental spectrum into the line components by a least-squares fitting procedure. The fit of 73 Voigt functions to the experimental spectrum is shown in Fig. 1. The energies of the lines obtained from the fit are given in Table I. For comparison, the energies reported by Werme *et al.*[1] are also tabulated applying the correction of 0.24 eV proposed by Ohtani *et al.*[15] and Hansen *et al.*[8,9] The energy-level structure of the final state, as evaluated by subtracting the initial-state energy, is depicted in Fig. 2 together with the energy-level structure of Xe III reported by Hansen *et al.*[8] and Hertz.[10]

The linewidth of 0.3 eV was obtained for the Auger lines from the fit of the experimental spectrum. This value also contains the spectrometer broadening. No attempt was done to determine the inherent linewidth.

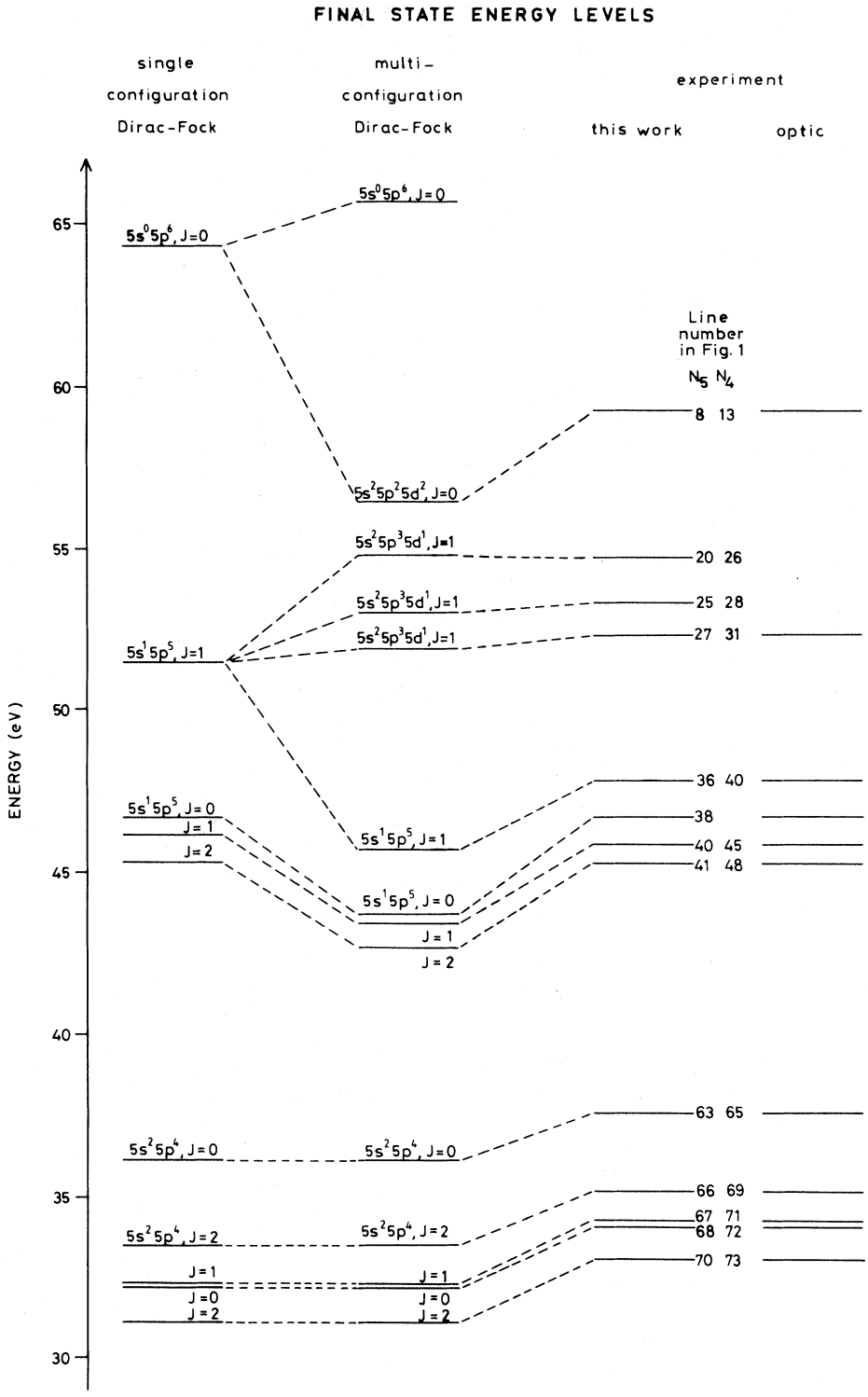

FIG. 2. Energy-level structure of doubly ionized xenon obtained from single and multiconfiguration Dirac-Fock calculations, Auger-electron spectroscopy, and optical spectroscopy. The designations in the multiconfiguration DF results refer to the configuration which makes a dominant contribution to the eigenvector.

III. DISCUSSION

In the studied energy region of 5—40 eV the observed fine structure is mainly due to the Auger transitions from the $4d^9 5s^2 5p^6$ initial state to the $4d^{10} 5s^0 5p^6$, $4d^{10} 5s^1 5p^5$, and $4d^{10} 5s^2 5p^4$ final states. Autoionization lines, where, instead of ionization, excitation of the electron takes place in the initial state, may accompany the Auger transitions.

Single configuration Dirac-Fock calculations were first carried out for all the states participating in the Auger

transitions, using the computer code of Grant *et al.*[1] The Auger energies were then obtained as a difference between the singly ionized initial-state and the doubly ionized final-state energies. Absolute energies of the initial-state (Xe II) and final-state (Xe III) levels were also obtained as an energy difference between the neutral and singly ionized atom, and the neutral and doubly ionized atom, respectively.

The experimental energies of the $N_{4,5}O_{2,3}O_{2,3}$ transitions were found to be lower by about 0.7 eV than the values calculated with the single configuration approximation. This difference arises from the deviations between experiment and theory both in the initial and in the final states. The energies of the $4d^9 5s^2 5p^6(^2D_{5/2})$ initial state were found to be 67.55 and 66.52 eV and the energies of the $4d^{10}5s^2 5p^4(^1D_2)$ final state were found to be 35.23 and 33.51 eV experimentally and theoretically, respectively. The calculated final-state energy levels are depicted together with the experimental results in Fig. 2. The $4d^{10}5s^2 5p^4$ final-state energy splitting seems to be slightly larger theoretically than experimentally, which is found to be a common tendency when calculated and experimental energy splittings are compared. However, the single configuration estimation seems to reproduce the observed energy-level structure of the $4d^{10}5s^2 5p^4$ configuration reasonably well.

In the case of the $N_{4,5}O_1O_1$ and $N_{4,5}O_1O_{2,3}$ transitions the situation seems to be completely different. A comparison between the experimental energies of the $N_{4,5}O_1O_{2,3}$ transitions and those calculated with the single configuration approach shows that the theoretical values are lower by 2.1 to 4.7 eV than the experimental energies. The normal Auger transitions are accompanied on their low-energy side by satellite lines caused by the process where the $5s$ hole is filled by a $5p$ electron with simultaneous excitations of another $5p$ electron to a $5d$ or $6s$ state. The marked discrepancy between the experiment and the single configuration estimations is caused by the neglect of the correlation between the final states of the normal and these satellite transitions. The near degeneracy of the two final-state configurations, as illustrated in Fig. 3, leads to a strong mixing between them, which then results in a redistribution of the intensity and a large energy shift of the lines. The configuration interaction ($5s5p^6 \leftrightarrow 5s^2 5p^4 5d$ or $5s^2 5p^4 6d$) was found to produce intense satellites in the photoelectron spectra.[6,7] In this work the correlation between the final states has been analyzed with the use of the multiconfiguration approach. The single and multiconfiguration results for the final-state energy levels are depicted together with the experimental results in Fig. 2. Table II shows the mixing of the single-configuration final-state wave functions. The intensity belonging to the $4d^9 \rightarrow 5s^0 5p^6$ and the $4d^9 \rightarrow 5s^1 5p^5$ transitions in the single-particle picture is now redistributed between the transitions to the final states of Table II. A comparison between the present multiconfiguration results and the experiment allows us to assign the fine structure of the Auger spectrum around 5–25 eV. Furthermore, we can compare our interpretation with the one offered by Southworth *et al.*[12] and Hansen *et al.*[8,9] Owing to the strong mixing of the final states by electron correlation, the single configuration assignment is no longer meaningful. Thus we do not label some lines to the normal and others to the satellite transitions, but prefer the atomic-state description of Table II for the final states of the transitions.

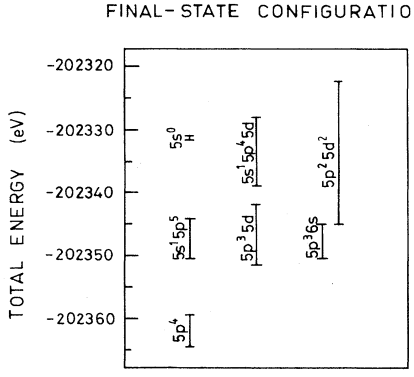

FIG. 3. Calculated energy positions of the final-state configurations of Auger and satellite transitions of xenon.

The lines at the 14.18 and 16.15-eV energies (lines 25 and 28 in Fig. 1), identified as the $N_{4,5}O_1O_1$, $^1S_0$ transitions by Werme *et al.*, should be reassigned as transitions with pronounced $5s^2 5p^3 5d^1$, $J=1$ final-state character. Our calculations thus support the same reinterpretation as was recently pointed out by Hansen *et al.*[8,9] and Southworth *et al.*[12] Apart from these lines, two other lines in both groups (lines 20 and 27 in the N_5 group and lines 26 and 31 in the N_4 group), containing a pronounced $5s^2 5p^3 5d^1$, $J=1$ final-state character, but also a notable $5s^1 5p^5$ amount, can be clearly identified in the experimental spectrum.

Two lines were obtained experimentally at energies of 8.30 and 10.27 eV (lines 8 and 13 in Fig. 1). These lines, identified as the $N_{4,5}O_1,O_1$, $^1S_0$ transitions by Hertz[10] Hansen *et al.*,[8,9] and Southworth *et al.*,[12] are found to be displaced by about 6.1 eV from the position expected on the basis of a single-particle approximation, and the perturbation responsible is the interaction of the $5s^0 5p^6$ final-state configuration with the $5s^1 5p^4 5d^1$ and $5s^2 5p^2 5d^2$ configurations. Owing to the distribution of the $5s^0 5p^6$ final state over the $5s^1 5p^4 5d^1$ and $5s^2 5p^2 5d^2$ states, several levels, each of which contain a certain amount of $5s^0 5p^6$ character, are obtained by the multiconfiguration approach. The Auger transitions whose energies are estimated to be 0.81 and 2.77 eV, for example, contain a considerably large amount of $5s^0 5p^6$ character. Owing to the strongly increasing background in going to lower energies, it has not been possible to observe these lines experimentally.

The multiconfiguration estimations do not agree very well with the experiment, as can be seen from Fig. 2 and Table II. In fact, it is clear that in order to arrive at a complete description of the energy-level structure, it is necessary to include the interaction with the continuum, as well as the other weaker interactions, both in the initial and in the final states. Satisfactory agreement between the present theoretical and experimental results, however, clearly indicates that the appearance of the observed

TABLE II. Experimental and calculated energies of the $4d$ Auger transitions of Xe.

Experimental						Calculated			
	Absolute energy			Relative energy		Absolute energy			
Line in Fig. 1	N_5	Line in Fig. 1	N_4	This work	Optic	N_5	N_4	Relative energy	Single configuration designation
						0.68	2.64	−32.33	
8	8.30	13	10.27	−24.01	−24.02	10.59	12.55	−22.42	$N_{4,5}O_1O_1(^1S_0)$
20	12.85	26	14.66	−19.46		11.74	13.70	−21.27	
25	14.18	28	16.15	−18.13		13.47	15.43	−19.54	
27	15.26	31	17.25	−17.05	−17.05	14.65	16.60	−18.36	
36	19.71	40	21.67	−12.60	−12.63	20.81	22.77	−12.20	$N_{4,5}O_1O_{2,3}(^1P_1)$
38	20.92			−11.39	−11.45	22.82	24.78	−10.19	$N_{4,5}O_1O_{2,3}(^3P_0)$
40	21.67	45	23.57	−10.64	−10.72	23.06	25.01	−9.95	$N_{4,5}O_1O_{2,3}(^3P_1)$
41	22.23	48	24.46	−10.08	−10.06	23.78	25.74	−9.23	$N_{4,5}O_1O_{2,3}(^3P_2)$
63	29.95	65	31.93	−2.36	−2.35	30.37	32.33	−2.64	$N_{4,5}O_{2,3}O_{2,3}(^1S_0)$
66	32.31	69	34.31	0.00	0.00	33.01	34.97	0.00	$N_{4,5}O_{2,3}O_{2,3}(^1D_2)$
67	33.24	71	35.20	0.93	0.91	34.25	36.21	1.24	$N_{4,5}O_{2,3}O_{2,3}(^3P_1)$
68	33.45	72	35.37	1.14	1.12	34.33	36.29	1.32	$N_{4,5}O_{2,3}O_{2,3}(^3P_0)$
70	34.46	73	36.41	2.15	2.12	35.43	37.39	2.42	$N_{4,5}O_{2,3}O_{2,3}(^3P_2)$

behavior mainly arises from the final-state configuration mixing which is related to the collapse of the $5d$ orbital at the beginning of the sequence. The $6s$ orbital seems to play a minor role in the present case.

A recent study of the energy-level structure of Xe III using optical spectroscopy[8–10] reports a wide variety of energy levels, which have not all, however, been identified in the Auger spectrum due to the low intensity of the transitions to these final states. The two sets of experimental results agree very well with each other in all the cases where comparison has been possible (see Table II and Fig. 2). In the case of the $N_{4,5}O_1O_{2,3}$ transitions, two lines in both groups (lines 20 and 25 in the N_5 and lines 26 and 28 n the N_4 group) with a pronounced $5s^25p^35d^1$ final-state character were clearly identified; no corresponding optical results are available because they are produced by final states at higher energies than those reported in the spectroscopic tables. With regard to the assignment of lines 25 and 28, we agree with Southworth *et al.*,[12] whereas line 27 at 15.26 eV energy was left unassigned by Southworth *et al.* An inspection of the final-state wave functions given in Table II shows a great amount of $5s^15p^5$, $J=1$ character for the lines at the energies of 14.65 and 16.60 eV. Thus an obvious transfer of the intensity is expected. Lines 27 and 31 should therefore be identified as the normal N_5 and N_4 transitions to the final state given in Table II. The relative intensities of the experimentally observed Auger and satellite transitions roughly seem to follow the squares of the mixing coefficients. However, no detailed intensity analysis or comparison between experiment and theory has been carried out, because the subtraction of the strongly increasing background at lower energies makes the determination of the intensity values inaccurate.

TABLE II. (*Continued*).

Wave function of the final state
$-0.57 \mid 5s^0\bar{5p}^2 5p^4, J=0\rangle - 0.24 \mid 5s^2\bar{5p}^1 5p^1 \bar{5d}^0 5d^2, J=0\rangle$
$-0.23 \mid 5s^1\bar{5p}^1 5p^3 \bar{5d}^1 5d^0, J=0\rangle + 0.40 \mid 5s^1\bar{5p}^1 5p^3 \bar{5d}^0 5d^1, J=0\rangle$
$+0.30 \mid 5s^1\bar{5p}^2 5p^2 \bar{5d}^1 5d^0, J=0\rangle - 0.44 \mid 5s^1\bar{5p}^2 5p^2 \bar{5d}^0 5d^1, J=0\rangle$
$0.41 \mid 5s^0\bar{5p}^2 5p^4, J=0\rangle - 0.20 \mid 5s^2\bar{5p}^0 5p^2 \bar{5d}^2 5d^0, J=0\rangle$
$-0.43 \mid 5s^2\bar{5p}^0 5p^2 \bar{5d}^1 5d^1, J=0\rangle + 0.33 \mid 5s^2\bar{5p}^0 5p^2 \bar{5d}^2 5d^0, J=0\rangle$
$-0.20 \mid 5s^2\bar{5p}^1 5p^1 \bar{5d}^1 5d^1, J=0\rangle + 0.26 \mid 5s^2\bar{5p}^1 5p^1 \bar{5d}^1 5d^1, J=0\rangle$
$-0.20 \mid 5s^2\bar{5p}^2 5p^0 \bar{5d}^2 5d^0, J=0\rangle + 0.22 \mid 5s^2\bar{5p}^0 5p^2 \bar{5d}^0 5d 6s^1, J=0\rangle$
$-0.20 \mid 5s^1\bar{5p}^1 5p^3 \bar{5d}^1 5d^0, J=0\rangle - 0.20 \mid 5s^1\bar{5p}^2 5p^2 \bar{5d}^1 5d^0, J=0\rangle$
$-0.23 \mid 5s^1\bar{5p}^0 5p^4 \bar{5d}^0 5d^0 6s^1, J=0\rangle + 0.24 \mid 5s^1\bar{5p}^2 5p^2 \bar{5d}^0 5d^0 6s^1, J=0\rangle$
$0.47 \mid 5s^1\bar{5p}^1 5p^4, J=1\rangle + 0.45 \mid 5s^1\bar{5p}^2 5p^3, J=1\rangle + 0.59 \mid 5s^2\bar{5p}^0 5p^3 \bar{5d}^0 5d^1, J=1\rangle$
$+0.32 \mid 5s^2\bar{5p}^1 5p^2 \bar{5d}^1 5d^0, J=1\rangle + 0.25 \mid 5s^2\bar{5p}^2 5p^1 \bar{5d}^0 5d^1, J=1\rangle$
$-0.33 \mid 5s^1\bar{5p}^1 5p^4, J=1\rangle - 0.38 \mid 5s^1\bar{5p}^2 5p^3, J=1\rangle + 0.43 \mid 5s^2\bar{5p}^0 5p^3 \bar{5d}^0 5d^1, J=1\rangle$
$+0.54 \mid 5s^2\bar{5p}^0 5p^3 \bar{5d}^1 5d^0, J=1\rangle + 0.22 \mid 5s^2\bar{5p}^1 5p^2 \bar{5d}^1 5d^0, J=1\rangle$
$+0.35 \mid 5s^2\bar{5p}^1 5p^2 \bar{5d}^0 5d^1, J=1\rangle + 0.21 \mid 5s^2\bar{5p}^2 5p^1 \bar{5d}^0 5d^1, J=1\rangle$
$0.34 \mid 5s^1\bar{5p}^1 5p^4, J=1\rangle - 0.42 \mid 5s^1\bar{5p}^2 5p^3, J=1\rangle + 0.39 \mid 5s^2\bar{5p}^0 5p^3 \bar{5d}^0 5d^1, J=1\rangle$
$-0.26 \mid 5s^2\bar{5p}^0 5p^3 \bar{5d}^1 5d^0, J=1\rangle - 0.33 \mid 5s^2\bar{5p}^1 5p^2 \bar{5d}^0 5d^1, J=1\rangle$
$+0.30 \mid 5s^2\bar{5p}^1 5p^2 \bar{5d}^0 5d^1, J=1\rangle + 0.43 \mid 5s^2\bar{5p}^1 5p^2 \bar{5d}^1 5d^0, J=1\rangle$
$-0.42 \mid 5s^1\bar{5p}^1 5p^4, J=1\rangle - 0.22 \mid 5s^1\bar{5p}^2 5p^3, J=1\rangle + 0.35 \mid 5s^2\bar{5p}^1 5p^2 \bar{5d}^0 5d^1, J=1\rangle$
$-0.20 \mid 5s^2\bar{5p}^1 5p^2 \bar{5d}^1 5d^0, J=1\rangle - 0.54 \mid 5s^2\bar{5p}^1 5p^2 \bar{5d}^0 5d^1, J=1\rangle + 0.22 \mid 5s^2\bar{5p}^2 5p^1 \bar{5d}^0 5d^1, J=1\rangle$
$+0.31 \mid 5s^2\bar{5p}^2 5p^1 \bar{5d}^1 5d^0, J=1\rangle - 0.34 \mid 5s^2\bar{5p}^2 5p^1 \bar{5d}^0 5d^0 6s^1, J=1\rangle$
$-0.66 \mid 5s^1\bar{5p}^1 5p^4, J=0\rangle - 0.59 \mid 5s^2\bar{5p}^1 5p^2 \bar{5d}^1 5d^0, J=0\rangle$
$+0.29 \mid 5s^2\bar{5p}^1 5p^2 \bar{5d}^0 5d^1, J=0\rangle - 0.36 \mid 5s^2\bar{5p}^2 5p^1 \bar{5d}^1 5d^0, J=0\rangle$
$-0.50 \mid 5s^1\bar{5p}^1 5p^4, J=1\rangle + 0.55 \mid 5s^1\bar{5p}^2 5p^3, J=1\rangle + 0.24 \mid 5s^2\bar{5p}^1 5p^2 \bar{5d}^0 5d^1, J=1\rangle$
$+0.35 \mid 5s^2\bar{5p}^1 5p^2 \bar{5d}^0 5d^1, J=1\rangle - 0.43 \mid 5s^2\bar{5p}^2 5p^1 \bar{5d}^1 5d^0, J=1\rangle$
$0.81 \mid 5s^1\bar{5p}^2 5p^3, J=1\rangle - 0.30 \mid 5s^2\bar{5p}^1 5p^2 \bar{5d}^0 5d^1, J=2\rangle + 0.22 \mid 5s^2\bar{5p}^1 5p^2 \bar{5d}^1 5d^0, J=2\rangle$
$+0.34 \mid 5s^2\bar{5p}^2 5p^1 \bar{5d}^0 5d^1, J=2\rangle$
$-0.84 \mid 5\bar{p}^0 5p^4, J=0\rangle - 0.54 \mid 5\bar{p}^2 5p^2, J=0\rangle$
$-0.95 \mid 5\bar{p}^1 5p^3, J=2\rangle + 0.31 \mid 5\bar{p}^2 5p^2, J=2\rangle$
$-1.00 \mid 5\bar{p}^1 5p^3, J=1\rangle$
$0.54 \mid 5\bar{p}^1 5p^3, J=0\rangle - 0.84 \mid 5\bar{p}^2 5p^2, J=0\rangle$
$0.31 \mid 5\bar{p}^1 5p^3, J=2\rangle + 0.95 \mid 5\bar{p}^2 5p^2, J=2\rangle$

Apart from the main lines labeled in Table II several low-intensity lines are observed experimentally (Fig. 1 and Table I). Multiconfiguration computations indicate several extra lines with relatively small amounts of $5s^0 5p^6$ and $5s^1 5p^5$ character. Identification of these lines with very small intensity is, however, difficult, because they are accompanied by several other lines: The autoionization lines with a $6p$ spectator electron[12] lie on the high-energy side of the main lines. The high-energy electron beam used can ionize the deeper M and N levels. Via the Auger decay, this may lead to doubly ionized states, where one of the holes is created in the $4d$ level. The satellite Auger transitions, when these double-hole states decay to the triple-hole states, fall energetically on the low-energy side of the normal Auger transitions. Thus the low-intensity lines are too numerous to investigate in full, which is why only the identification of the major lines has been presented.

ACKNOWLEDGMENT

This work was supported by the Finnish Academy of Science.

[1]L. O. Werme, T. Bergmark, and K. Siegbahn, Phys. Scr. 6, 141 (1972).
[2]E. J. McGuire, Phys. Rev. A 11, 1880 (1975).
[3]E. J. McGuire, Phys. Rev. A 11, 17 (1975).
[4]K. G. Dyall and F. P. Larkins, J. Phys. B 15, 2793 (1982).
[5]K. G. Dyall and F. P. Larkins, in *Inner-shell and x-Ray, Physics of Atoms and Solids,* edited by D. J. Fabian, H. Kleinpoppen, and M. Watson (Plenum, New York, 1981), p. 265.
[6]M. Y. Adam, F. Wuilleumier, N. Sandner, W. Schmidt, and G. Wedin, J. Phys. (Paris) 39, 129 (1978).
[7]J. E. Hansen and W. Persson, Phys. Rev. A 18, 1459 (1978).
[8]J. E. Hansen and F. G. Meijer, Phys. Scr. (to be published).
[9]J. E. Hansen, Phys. Scr. 25, 487 (1982).
[10]H. Hertz, Z. Phys. A 247, 289 (1975).
[11]I. P. Grant, B. J. Kenzie, and P. H. Norrington, Comput. Phys. Comm. 21, 207 (1980); *ibid.* 21, 233 (1980).
[12]S. Southworth, V. Becker, C. M. Truesdale, P. H. Kobrin, D. W. Lindle, S. Owaki, and D. A. Shirley, Phys. Rev. A 28, 261 (1983).
[13]J. Väyrynen and S. Aksela, J. Electron Spectrosc. 16, 423 (1979).
[14]G. King, M. Trone, F. Read, and R. Brandford, J. Phys. B 10, 2479 (1977).
[15]S. Ohtani, N. Nishimura, and H. Suzuki, Phys. Rev. Lett. 36, 863 (1976).